

Low energy physics from the QCD Schrödinger functional*

Joyce Garden^a, Marco Guagnelli^b, Jochen Heitger^c, Rainer Sommer^c and Hartmut Wittig^{d†}

(ALPHA and UKQCD Collaborations)

^a Department of Physics & Astronomy, University of Edinburgh, Edinburgh EH9 3JZ, Scotland

^b Dipartimento di Fisica, Università di Roma *Tor Vergata*, and INFN, Sezione di Roma II

^c Deutsches Elektronen-Synchrotron DESY Zeuthen, Platanenallee 6, D-15738 Zeuthen, Germany

^d Theoretical Physics, University of Oxford, 1 Keble Road, Oxford OX1 3NP, UK

We review recent work by the ALPHA and UKQCD Collaborations where masses and matrix elements were computed in lattice QCD using Schrödinger functional boundary conditions and where the strange quark mass was determined in the quenched approximation. We emphasize the general concepts and our strategy for the computation of quark masses.

1. Introduction

Based on the recent progress in lattice QCD concerning non-perturbative renormalization of local composite operators and removal of leading discretization errors [1–3], there is a natural interest to calculate hadron masses and matrix elements in the continuum limit. Especially, the problem of a determination of the light quark masses [4] can be addressed with confidence, since the complete renormalization is known non-perturbatively [5,6].

As an alternative to more standard methods, we will show that the Schrödinger functional (SF) framework allows for a reliable computation of spectral quantities with high accuracy in lattice QCD. As a necessary prerequisite, we will demonstrate explicitly that SF correlation functions are dominated by hadron intermediate states at Euclidean time separations of around 3 fm.

This technique is then applied to physical observables in the meson sector of QCD, in particular to light quark masses. We present an overview of the work discussed in refs. [7,8]. All results refer to the fully $O(a)$ improved theory, but due to the rather introductory character all issues re-

lated to $O(a)$ improvement are ignored here.

Our quenched data stem from four lattices (SF boundary conditions) of spatial extent $L \approx 1.5$ fm and time extension $T = 2L$ with lattice spacings, a , from 0.1 fm ($\beta = 6.0$) to 0.05 fm ($\beta = 6.45$), and with four values of the quark mass each, so that all results can be extrapolated first in the pseudoscalar mass and finally to the continuum limit. For our choice of parameters, chiral perturbation theory predicts negligible finite size effects and an explicit investigation [8], which is not discussed here, confirms this.

2. SF correlators at large time separations

The SF is defined as the QCD partition function in a $L^3 \times T$ cylinder with periodic boundary conditions in three of the four Euclidean dimensions and Dirichlet boundary conditions in time at the hypersurfaces $x_0 = 0$ and $x_0 = T$ [9]. Whereas in earlier applications, e.g. in refs. [5,6], correlation functions in the SF were mainly considered in the perturbative regime (i.e. small extensions of the space-time volume), the emphasis in this section is on their properties in intermediate to large volumes with extensions significantly larger than the typical QCD scales of order 1 fm.

Starting from the quantum mechanical interpretation of the SF [9,10], one can derive explicit

*based on talks given by J. H. and R. S. at the conference LATTICE '99, June 29 – July 3, 1999, in Pisa, Italy

†PPARC Advanced Fellow

expressions for the representation of its correlation functions in terms of intermediate physical states [7]. Let us discuss an example which is directly relevant in section 3. We consider the correlation functions

$$f_X(x_0) = -\frac{L^3}{2} \langle X(x) \mathcal{O} \rangle, \quad (1)$$

$$f_1 = -\frac{1}{2} \langle \mathcal{O}' \mathcal{O} \rangle, \quad (2)$$

where \mathcal{O} is a pseudoscalar field, constructed from a $\mathbf{p} = 0$ quark field and a $\mathbf{p} = 0$ antiquark field at $x_0 = 0$: $\mathcal{O} = \frac{a^6}{L^3} \sum_{\mathbf{y}, \mathbf{z}} \bar{\zeta}_i(\mathbf{y}) \gamma_5 \zeta_j(\mathbf{z})$, i, j being flavor indices. Analogously, \mathcal{O}' is located at the boundary $x_0 = T$. One may think of the fields ζ, \dots as quark fields at the boundary; their precise definition is given in [11]. In the following, we shall be interested in f_A , defined by $X(x) = A_0(x) = \bar{\psi}_j(x) \gamma_0 \gamma_5 \psi_i(x)$, and f_P , given by $X(x) = P(x) = \bar{\psi}_j(x) \gamma_5 \psi_i(x)$.

For large separations x_0 and $T - x_0$ the correlation functions are dominated by the lowest lying intermediate states with the appropriate quantum numbers. These are the pseudoscalar ground state and the vacuum, the latter contributing between x_0 and T in both f_A and f_P . In the transfer matrix formalism one may then arrive [7] at the asymptotic behaviour including the first non-leading corrections:

$$\begin{aligned} f_X(x_0) &\approx \frac{L^3}{2} \rho \langle 0, 0 | \mathbb{X} | 0, \text{PS} \rangle e^{-x_0 m_{\text{PS}}} \\ &\quad \times \left\{ 1 + \eta_X^{\text{PS}} e^{-x_0 \Delta} + \eta_X^0 e^{-(T-x_0) m_G} \right\} \\ f_1 &\approx \frac{1}{2} \rho^2 e^{-T m_{\text{PS}}}. \end{aligned} \quad (3)$$

In leading order an unknown matrix element ρ and the desired matrix elements of the Schrödinger picture operators \mathbb{X} , associated with the fields X , arise. The mass of the 0^{++} glueball, m_G , and the gap in the pseudoscalar channel, Δ , enter the corrections with coefficients $\eta_X^0, \eta_X^{\text{PS}}$ expressed through certain matrix elements. Apart from the pseudoscalar mass, m_{PS} , the formulae (3) enable to calculate the decay constant, F_{PS} , and the pseudoscalar coupling, G_{PS} , via

$$\langle 0, 0 | \mathbb{A}_0 | 0, \text{PS} \rangle = F_{\text{PS}} m_{\text{PS}} (2m_{\text{PS}} L^3)^{-1/2}, \quad (4)$$

$$\langle 0, 0 | \mathbb{P} | 0, \text{PS} \rangle = G_{\text{PS}} (2m_{\text{PS}} L^3)^{-1/2}. \quad (5)$$

Note in particular that f_1 may be used to eliminate the unknown factor ρ , the only place where

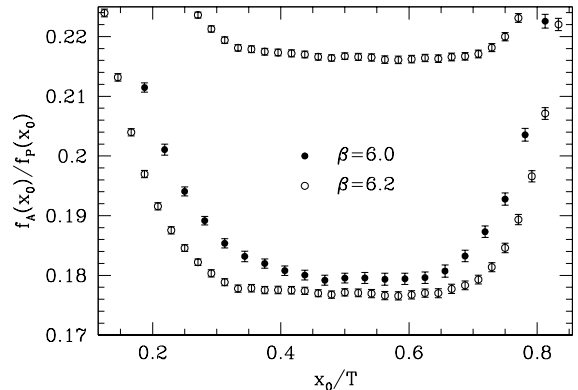


Figure 1. The ratio f_A/f_P for $a \approx 0.07$ fm (open circles) and $a \approx 0.09$ fm (filled circles).

the divergent renormalizations of the boundary quark fields are hidden. A generalization e.g. to the vector meson channel is straightforward.

We turn to the numerical tests of the practicality of our method. As a representative example, which moreover will play a crucial rôle in the next section, we discuss the ratio

$$\frac{f_A}{f_P} = \frac{m_{\text{PS}} F_{\text{PS}}}{G_{\text{PS}}} \left\{ 1 + \mathcal{O} \left(e^{-x_0 \Delta}, e^{-(T-x_0) m_G} \right) \right\}.$$

It shows approximate plateaux between $x_0 \approx 1$ fm and $T - x_0 \approx 1$ fm (Fig. 1). Their height determines $m_{\text{PS}} F_{\text{PS}} / G_{\text{PS}}$. Before, however, just reading these off, the magnitude of the “contaminations” by excited state contributions should be assessed. Given the fact that estimates for Δ and m_G are available [7], this may be achieved by plotting the ratio against the leading corrections: the slopes in Fig. 2 allow to deduce the range $t_{\text{min}} \leq x_0 \leq t_{\text{max}}$ where the excited state corrections are below a certain systematic error margin, which we chose in turn to be negligible compared to the final statistical errors. The ratio was then averaged in the range $t_{\text{min}} \leq x_0 \leq t_{\text{max}}$.

This procedure is easily extended to the calculation of m_{PS} , F_{PS} and G_{PS} separately.

The numerical efficiency of the computations with SF correlation functions is illustrated in Fig. 3, where we compare our results for the bare (improved) pseudoscalar decay constant with those found in the literature. To judge the relative size of the statistical errors one should note

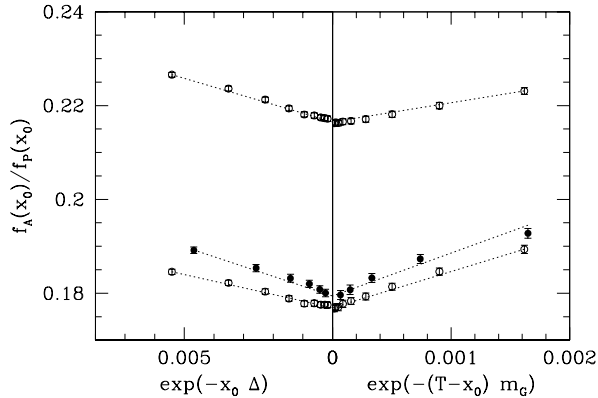


Figure 2. Influence of excited state contributions on f_A/f_P at the same parameters as in Fig. 1.

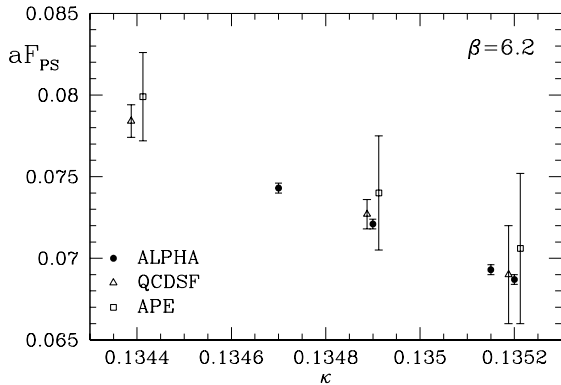


Figure 3. Comparison of some of our results (ALPHA) with those of the QCDSF [12] and APE [13] Collaborations. Symbols are slightly displaced.

that our statistics is not much higher than the statistics present in the other simulations.

Clearly, the SF applied for extracting hadron physics is similar to the method of wall sources, but one should note that gauge invariance is kept at all stages of the present formulation. Furthermore, dimensionless non-local fields are used to create the boundary states. Dimensional analysis then tells us that the pre-asymptotic decay of SF correlation functions is slow, leaving large and precise signals at hadronic length scales of 1-2 fm. Since the correlation functions are renormalizable by simple factors, this property is indeed independent of the lattice spacing, once one is sufficiently

close to the continuum limit.

3. Quark masses: the strategy

Before we come to the numerical applications of the above methods, we want to explain in detail our strategy for the computation of light quark masses. Their ratios can be computed from chiral perturbation theory [14]. The currently best results read

$$M_u/M_d = 0.55 \pm 0.04, \quad M_s/\hat{M} = 24.4 \pm 1.5 \quad (6)$$

with $\hat{M} = \frac{1}{2}(M_u + M_d)$ [15].

Despite this success, there is substantial work to be done using lattice QCD.

- The applicability of chiral perturbation theory needs to be checked. This concerns the practical question in how far the lowest orders dominate the full result.
- The parameters in the chiral Lagrangian (at a given order in the expansion) can not be inferred with great precision from experimental data alone. Their determination can be improved significantly by help of lattice QCD results.
- In particular, there is one parameter in the chiral Lagrangian which is impossible to determine from experimental data. This is the overall scale of the quark masses, which is only defined once the connection with the fundamental theory, QCD, is made.

An important point to realize is that all of the above problems can be dealt with by working with *unphysical quark masses* (of course they should not be too large). For the first two problems it is in fact essential to explore a range of quark masses, and also for the last problem, which we address here, this is of significant advantage.

The above considerations lead us to determine an implicitly defined reference quark mass M_{ref} ,

$$m_{\text{PS}}^2(M_{\text{ref}})r_0^2 = 1.5736 = (m_K r_0)^2, \quad (7)$$

where $m_{\text{PS}}^2(M)$ is the pseudoscalar meson mass as a function of the quark mass (mass-degenerate

quarks). Chiral perturbation theory *in full QCD* relates M_{ref} to the other light quark masses viz.

$$2M_{\text{ref}} \approx M_s + \hat{M}. \quad (8)$$

Further evidence for this relation is given in [8], using the results of quenched lattice QCD.

What was said above is valid literally in mass-independent renormalization schemes, where quark masses are renormalized with a flavor independent factor. The resulting running quark masses, $\bar{m}(\mu)$, are however scheme- and scale-dependent quantities. It is advantageous to compute directly the renormalization group invariant (RGI) quark masses [6], which are pure numbers and do not depend on the scheme. In terms of $\bar{m}(\mu)$ they are given as

$$M \equiv \lim_{\mu \rightarrow \infty} \left\{ (2b_0 \bar{g}^2(\mu))^{-d_0/2b_0} \bar{m}(\mu) \right\}, \quad (9)$$

$$b_0 = 11/(4\pi)^2, \quad d_0 = 8/(4\pi)^2. \quad (10)$$

For $O(a)$ improved quenched QCD, the ALPHA Collaboration has determined the renormalization factor Z_M relating the bare current quark masses m , defined by the PCAC relation, to the RGI masses [5,6]:

$$M = Z_M m. \quad (11)$$

Applying the PCAC relation to the vacuum-to-pseudoscalar matrix elements then results directly in our central relation,

$$2r_0 M_{\text{ref}} = Z_M \frac{R|_{r_0^2 m_{\text{PS}}^2 = 1.5736}}{r_0} \times 1.5736, \quad (12)$$

$$R = F_{\text{PS}}/G_{\text{PS}}. \quad (13)$$

4. Results

With the methods of section 2, the ratio R/a and the meson mass $m_{\text{PS}}a$ can be computed accurately as a function of the bare quark mass and the bare coupling. Also the scale r_0/a is known [16]. A mild extrapolation, shown in Fig. 4, then yields R/a at the point $r_0^2 m_{\text{PS}}^2 = 1.5736$.³ Next the full combination $r_0 M_{\text{ref}}$ (see eqs. (7,8)) is

³ The reason for not computing directly at or below the quark mass corresponding to $r_0^2 m_{\text{PS}}^2 = 1.5736$ was that this is the region where unphysical zero modes of the $O(a)$ improved Dirac operator are relevant (“exceptional configurations”).

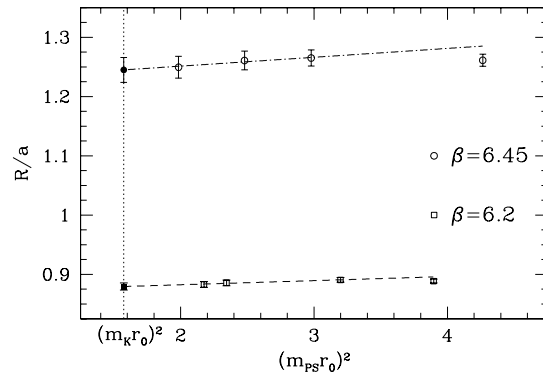


Figure 4. Mass dependence and extrapolations at the two smallest values of the lattice spacing.

extrapolated to the continuum limit in Fig. 5a. Since this latter extrapolation involves a significant slope we discarded the point furthest away from the continuum. This is a safeguard against higher order lattice spacing effects.

Furthermore, the entire analysis was repeated for M_{ref} in units of the Kaon decay constant [8]. In this case the lattice spacing dependence is weaker (Fig. 5b). The two results,

$$2r_0 M_{\text{ref}} = 0.36(1)$$

$$\xrightarrow{r_0 = 0.5 \text{ fm}} 2M_{\text{ref}} = 143(5) \text{ MeV},$$

$$2M_{\text{ref}}/(F_{\text{K}})_{\text{R}} = 0.87(3)$$

$$\xrightarrow{(F_{\text{K}})_{\text{R}} = 160 \text{ MeV}} 2M_{\text{ref}} = 140(5) \text{ MeV},$$

agree better than one would expect them to do in the quenched approximation.

It is premature to conclude that this approximation yields a nearly unique result. Rather, the assignment of physical units *is* ambiguous. One may estimate [8] by help of the recent results of the CP-PACS Collaboration [18] that roughly 10% larger numbers would be obtained, if the scale r_0 were replaced by one of the masses of the stable light hadrons. This represents a typical ambiguity of the quenched approximation.

It is now understood that this technical problem can be resolved by introducing the quark mass into the lattice theory in a particular way [17]. However, even without entering this region, our quark mass points are close enough to perform a safe extrapolation.

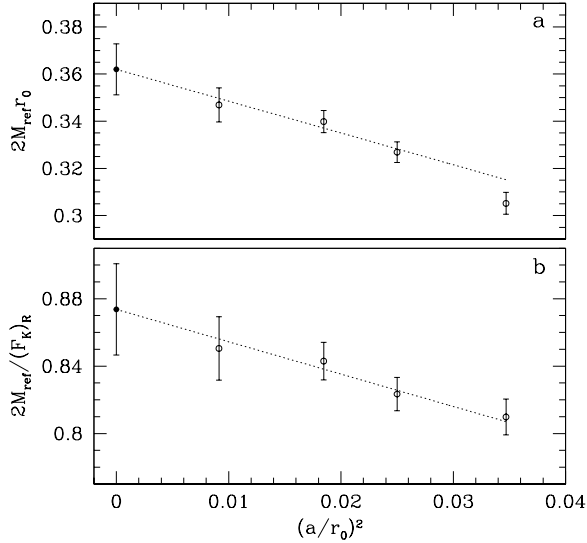


Figure 5. Continuum extrapolations of M_{ref} in units of r_0 (a) and $(F_K)_R$ (b). Full symbols are the $a = 0$ limits. The (dashed) fit functions are continued beyond their range towards larger a .

Other interesting results after extrapolation to the continuum limit are

$$\{r_0(F_{\text{PS}})_R\}_{r_0^2 m_{\text{PS}}^2 = 1.5736} = 0.415(9)$$

compared to $0.5 \text{ fm} \times (F_K)_R = 0.405(5)$ with the experimental value of $(F_K)_R$, and

$$\{r_0 m_{\text{vector}}\}_{r_0^2 m_{\text{PS}}^2 = 1.5736} = 2.39(7)$$

to be confronted with $0.5 \text{ fm} \times m_{K^*} = 2.26$. In the latter comparison one should remember that the K^* meson is unstable even in absence of electroweak interactions. Its width, Γ_{K^*} , amounts to $0.5 \text{ fm} \times \Gamma_{K^*} = 0.13$.

5. Discussion

In addition to the – by now well known – applications to renormalization problems in QCD, the Schrödinger functional has been shown to be useful for the computation of low energy matrix elements. For the particular cases of vacuum-to-pseudoscalar matrix elements, our results are significantly more precise than those from standard methods. This implies a precise computation (in the continuum limit) of the renormalization

group invariant quark mass M_{ref} defined above. $\overline{\text{MS}}$ masses for finite renormalization scales μ are obtained through perturbative conversion factors known up to 4-loop precision. A typical result is

$$\overline{m}_s(2 \text{ GeV}) = 97(4) \text{ MeV},$$

where the uncertainty in $\Lambda_{\overline{\text{MS}}}^{(0)} = 238(19) \text{ MeV}$ [6], entering the relation of the running quark masses in the $\overline{\text{MS}}$ scheme to the RGI masses, has been accounted for and the quark mass ratios from full QCD chiral perturbation theory were used.

One should keep in mind that there is an intrinsic ambiguity when assigning physical units in the quenched approximation. We estimated this to be of order 10%.

REFERENCES

1. Y. Kuramashi, these proceedings.
2. R. Sommer, Nucl. Phys. Proc. Suppl. 60A (1998) 279, hep-lat/9705026.
3. H. Wittig, Nucl. Phys. Proc. Suppl. B63 (1998) 47, hep-lat/9710013.
4. R.D. Kenway, Nucl. Phys. Proc. Suppl. B73 (1999) 16, hep-lat/9810054.
5. S. Sint and P. Weisz, Nucl. Phys. B545 (1999) 529, hep-lat/9808013.
6. S. Capitani, M. Lüscher, R. Sommer and H. Wittig, Nucl. Phys. B544 (1999) 669, hep-lat/9810063.
7. M. Guagnelli, J. Heitger, R. Sommer and H. Wittig, (1999), hep-lat/9903040.
8. J. Garden, J. Heitger, R. Sommer and H. Wittig, (1999), hep-lat/9906013.
9. M. Lüscher et al., Nucl. Phys. B384 (1992) 168, hep-lat/9207009.
10. S. Sint, Nucl. Phys. B421 (1994) 135, hep-lat/9312079.
11. M. Lüscher, S. Sint, R. Sommer and P. Weisz, Nucl. Phys. B478 (1996) 365, hep-lat/9605038.
12. M. Göckeler et al., Phys. Rev. D57 (1997) 5562, hep-lat/9707021.
13. D. Becirevic et al., (1998), hep-lat/9809129.
14. J. Gasser and H. Leutwyler, Phys. Rept. 87 (1982) 77.
15. H. Leutwyler, Phys. Lett. B378 (1996) 313, hep-ph/9602366.

16. M. Guagnelli, R. Sommer and H. Wittig, Nucl. Phys. B535 (1998) 389, hep-lat/9806005.
17. R. Frezzotti, P.A. Grassi, S. Sint and P. Weisz, these proceedings, hep-lat/9909003.
18. S. Aoki et al., (1999), hep-lat/9904012.